Published in final edited form as:
Cell. 2011 February 18; 144(4): 526–538. doi:10.1016/j.cell.2011.02.005.

ATP binds to proteasomal ATPases in pairs with distinct functional effects implying an ordered reaction cycle

David M. Smith[*,‡], **Hugo Fraga**, **Christian Reis**, **Galit Kafri**, and **Alfred L. Goldberg**[*]
Department of Cell Biology, Harvard Medical School, 240 Longwood Avenue, Boston, MA 02115, USA.

Abstract

In the eukaryotic 26S proteasome, the 20S particle is regulated by six AAA ATPase subunits, and in archaea by a homologous ring complex, PAN. To clarify the role of ATP in proteolysis, we studied how nucleotides bind to PAN. Although PAN has six identical subunits it binds ATPs in pairs, and its subunits exhibit three conformational states with high, low, or no affinity for ATP. When PAN binds two ATPγS molecules, or two ATPγS plus two ADP molecules it is maximally active in binding protein substrates, associating with the 20S particle, and promoting 20S gate-opening. However, binding of four ATPγS molecules reduces these functions. The 26S proteasome shows similar nucleotide dependence. These findings imply an ordered cyclical mechanism in which two ATPase subunits bind ATP simultaneously and dock into the 20S. These results can explain how these hexameric ATPases interact with and "wobble" on top of the heptameric 20S proteasome.

Introduction

Intracellular protein degradation is an ATP-dependent process that is catalyzed primarily by the 26S proteasome in eukaryotic cells and by the PAN-20S proteasome in archaea (Glickman and Ciechanover, 2002; Goldberg, 2005). These proteolytic complexes contain a hollow barrelshaped 20S particle which contains multiple proteolytic sites sequestered inside its central chamber (Groll et al., 1997; Lowe et al., 1995). This compartmentalization of the active sites prevents nonspecific degradation of cellular proteins and allows highly selective protein degradation through regulation of the entry of substrates into the particle. In eukaryotic cells, this process generally requires ubiquitination of substrates, leading to their selective binding to the 19S regulatory particle, which associates with the 20S to form the 26S proteasome. The entry of protein substrates into the degradation chamber is facilitated in eukaryotes and archaea by hexameric ATPase complexes that associate with the outer ring of the 20S proteasome. These ATPase complexes are members of the AAA family of ATPases, and use ATP to catalyze substrate unfolding and translocation into the 20S (Smith et al., 2007; Zhang et al., 2009b). This process requires ATP binding or hydrolysis at multiple steps in order to facilitate substrate entry into the 20S particle and to overcome the steric barriers imposed by the architecture of the proteasome and the structure

[*]**Corresponding authors:** alfred_goldberg@hms.harvard.edu, david_smith@hms.harvard.edu.
[‡]Current Address: Department of Biochemistry, West Virginia University School of Medicine, Morgantown, WV, Tel: 617-432-1855

of the folded substrate (see below). Due to the importance of these ATPases, detailed knowledge about how they utilize ATP in these multiple steps is essential to understand how the proteasome catalyzes efficient protein degradation.

The 20S proteasome is composed of 28 subunits arranged in 4 stacked heptameric rings (Groll et al., 1997; Lowe et al., 1995). In the eukaryotic 20S, seven distinct (but homologous) β-subunits comprise the two identical inner rings and contain the proteolytic active sites, while seven distinct α-subunits comprise the two outer rings. The 20S proteasomes from archaea have similar structures, but its 7α subunits are identical as are its 7β subunits. Protein substrates can only enter and peptide products can only exit the 20S particle through a narrow 13Å translocation channel at the center of the α rings. Due to its small diameter, substrates must be unfolded and linearized before they can thread through this pore and enter the central degradation chamber. Substrate entry is tightly regulated and is normally blocked by the N-termini of the α subunits, which interact to form a gate.

To stimulate degradation by the 20S proteasome, the ATPases in the 19S particle or the homologous archaeal PAN ATPase complex serve five essential functions: they 1) associate with the 20S particle, 2) selectively bind the substrate, 3) cause the gated substrate-entry channel in the 20S to open, 4) unfold globular or partially folded proteins, and 5) facilitate the translocation of the unfolded substrate through the ATPase ring into the 20S particle. The substrate unfolding step is the only step in this process that actually requires ATP hydrolysis (Smith et al., 2006; Smith et al., 2005), while the other steps can be supported by ATP binding alone.

Several different types of models have been proposed for nucleotide binding and exchange for the different AAA+ ATPases (Augustin et al., 2009; Briggs et al., 2008; Hersch et al., 2005; Singleton et al., 2000). In principle, these hexamers may function in a concerted manner (e.g. where all subunits bind, hydrolyze, and then release nucleotides simultaneously) or in a non-concerted manner, in which the different subunits within the ring bind and hydrolyze nucleotides at distinct times (Ogura and Wilkinson, 2001). Such a binding-exchange reaction requires an allosteric system whereby different subunits regulate each other's behavior. Up to four different nucleotide states have been observed for a single AAA subunit: 1) ATP bound, 2) a transition state where ADP-Pi is bound, 3) ADP bound, 4) no nucleotide bound. Presumably, each of these states affects the conformation and function of the neighboring subunits in a distinct fashion so that ATP hydrolysis occurs in a non-concerted or sequential manner around the hexameric ring. However, it has also been demonstrated that a highly modified AAA+ ATPase (i.e. ClpX) can hydrolyze ATP in a non-cyclical fashion suggesting that non-patterned or stochastic hydrolysis is possible (Martin et al., 2005). These different ATPases are difficult to study quantitatively because the different states of the subunits are highly dynamic and are often heterogeneous. One valuable approach has been to use non-hydrolysable analogs of ATP to freeze the active, ATP-bound state, or ADP to capture the ATPase in the inactive conformation. If non-hydrolysable nucleotides can bind to only some of the six subunits, it would rule out concerted mechanisms that require simultaneous nucleotide binding to all subunits, and a completely stochastic mechanism whereby subunits could behave independently of one another.

The PAN-20S complex offers many advantages for studying the roles of ATP to help understand the functioning of the 26S proteasome. Although the 19S particle contains six different (but homologous) ATPases, PAN, like nearly all other AAA ATPases, is a hexameric ring composed of identical ATPase subunits. Although binding of ATPγS to PAN is sufficient to support its association with the 20S as well as opening of the gated 20S channel (Smith et al 2005), the number of nucleotide molecules that must bind to induce

complex formation and gate-opening is unknown. PAN and several of the 19S ATPase subunits contain an essential "HbYX" motif on their C-termini that upon ATP binding docks into pockets in the 20S α-ring and functions like "keys in a lock" to stimulate gate-opening. Peptides corresponding to the ATPases' C-termini that contain this motif can bind similarly and by themselves trigger gate-opening (Smith et al., 2007, Rabl et al., 2008).

Because ATP binding is required for these ATPase-20S interactions, it's very likely that the subunits that bind ATP (or ATPγS) are the ones whose C-termini dock into these pockets. If nucleotides bind to only some of the six ATPases (e.g. in a non-concerted binding-exchange reaction), then only a fraction of the ATPases C-termini may dock into the 20S proteasome at any one time. Therefore, determining the stoichiometry and interdependence of nucleotide binding to the six ATPases may help us to understand another fundamental mystery about the proteasome—how the hexameric ATPases' six C-termini can interact with and regulate the heptameric 20S proteasome (the "symmetry mismatch" problem).

Results

ATP dependence of protein and peptide degradation by the PAN-20S complex

To determine how the concentration of ATP influences PAN's capacity to stimulate degradation of different types of substrates by the archaeal proteasome, we assayed the degradation of: 1) a fluorogenic nonapeptide substrate, LFP (Fig. 1 B), whose hydrolysis requires only gateopening (Smith et al., 2005); 2) the inherently unstructured protein, β-casein (Fig. 1 C), and 3) the tightly folded globular protein, GFP-ssrA (Fig. 1 D). While the degradation of all these substrates is stimulated by ATP, the degradation of peptides and unfolded proteins does not require ATP hydrolysis but only ATP binding (i.e. it is supported by ATPγS), while the degradation of GFP-SsrA requires ATP hydrolysis for unfolding, (Benaroudj and Goldberg, 2000;Smith et al., 2005). Nevertheless, we found that very similar concentrations of ATP were required to support the degradation of each of these substrates. Specifically, the concentration of ATP to support half-maximal degradation rate (Kobs) for LFP was 233μM, for ^{14}C-casein 224μM, and for GFP-SsrA 302 μM.

When rates of ATP hydrolysis by PAN were measured, the Km for ATP was 263 +/− 18 μM (Fig. 1A). This value resembles closely the ATP concentrations that support half-maximal rates of proteolysis, even breakdown of peptides and unfolded proteins, which requires only ATP binding. The likely explanation for this agreement is that the duration of the ATP bound state is limited by how quickly the bound ATP is hydrolysed to ADP, which causes a loss of affinity of PAN for the 20S and gate-closing. Thus, binding of a new ATP is required to maintain this active complex. Because ATP must bind to be hydrolyzed, an increase in the rate of ATP hydrolysis (with increasing concentrations of ATP) implies that there must also be an increase in the fraction of subunits with ATP bound. Accordingly, the extent of 20S gate-opening, directly correlates with the rate of ATP hydrolysis in a linear fashion with an excellent fit (R^2=0.998). These arguments predict that ATPγS, which maintains PAN in the ATP-bound form, should be more efficient than ATP in stimulating peptide degradation, as we observed previously (Smith et al., 2005). Thus, although ATP hydrolysis to ADP diminishes PAN's ability to stimulate gate-opening, binding of a new ATP molecule stabilizes the PAN-20S complex, maintaining the gate in an open state.

PAN binds a maximum of 4 nucleotides per ring

Since each of PAN's and the 19S's six ATPases subunits contains a single Walker A and B ATPase domain, nucleotides may bind the hexamer in a number of possible configurations. For other members of the AAA family, different numbers of nucleotides bound per hexameric ring have been reported. To determine the actual number of nucleotides that PAN

binds at different concentrations, we incubated PAN with increasing concentrations of ^{32}P-ATP. A rapid spin gel filtration (G50) was used to quickly separate PAN and the bound nucleotide from the free nucleotide. The amount of recovered protein and the amount of bound radioactive ligand were quantified and used to calculate the number of nucleotides bound per hexamer (Menon and Goldberg, 1987). PAN bound a maximum of only four ATP molecules per hexamer (Fig 2A), even at saturating concentrations of ATP. This result is consistent with observations for other AAA family members where substoichiometric binding of nucleotides to the hexameric ring was also observed (Horwitz et al., 2007). The observed K_d for nucleotide binding was 13 μM, which is significantly lower than the K_M observed for PAN's ATPase activity, for gate-opening, and for proteolysis (224–302 μM). Since ATP is hydrolyzed to ADP, this effective Kd value must primarily reflect the combined on-rates of ATP and the off-rates for ADP.

Bound ATP is rapidly hydrolyzed, even at 4°C, and ADP remains bound

To determine the nature of the nucleotide that is bound to PAN after incubation with ^{32}P-ATP, we isolated PAN with bound nucleotides and used thin layer chromatography to analyse the eluate. When the binding reaction and isolation were carried out at 25° or even at 4°C, we could only detect ADP bound to PAN (Fig 2B). This result was surprising since ATP hydrolysis by PAN cannot be detected at either of these temperatures (data not shown). Therefore, even at 4°C, PAN rapidly catalyzes a single round of ATP hydrolysis, after which the ADP remains tightly bound.

Because only four ADP were bound at saturating ATP concentrations, we tested by a similar method if PAN could bind more ADP when it was added at saturating concentrations (Fig 2B). Even at 500 μM ^{14}C-ADP, the PAN hexamer still only bound four ADP molecules per hexamer, suggesting that a negative allostery prevents binding to two of PAN's subunits. Because we measured ATP binding using α-^{32}P-ATP, the presence of the bound ^{32}P-ADP did not indicate whether the generated Pi moiety remained bound to PAN. We therefore carried out a similar experiment with γ-^{32}P-ATP to follow the fate of ^{32}P. No radioactivity was eluted with PAN nor were there any other ^{32}P-spots on the thin layer chromatograph (data not shown). Thus, in contrast to the ADP, the free Pi moiety is released by PAN quickly after ATP hydrolysis.

ATPγS binding induces three different subunit conformations in PAN

Because PAN rapidly hydrolyzes ATP to ADP even at 4°C, we used the non-hydrolysable analog, ATPγS, to measure the stoichiometry of ATP binding. Using the same technique, we isolated PAN bound to ^{35}S-ATPγS at different ATPγS concentrations (Fig 3A). Although the binding curves for ATP showed typical saturation kinetics, surprisingly, the binding curve for ATPγS was multiphasic with two clear saturation plateaus (Fig 3A). This result indicates that the PAN homohexamer contains at least two distinct types of ATPγS-binding sites, one type with high-affinity (Kd=~0.493μM) and one with low-affinity (Kd=~113μM). Moreover, when the number of nucleotides bound was calculated, we found that only two nucleotides bound to the high affinity site (2-bound state) and two more nucleotides bound to the low-affinity sites (4-bound state). Since PAN is composed of six identical subunits around a ring, this result implies that binding of ATP to the high affinity subunit(s) induces a conformational change in the other subunits that decreases their affinity for nucleotides and reduces or prevents ATPγS binding. Thus, PAN subunits must exist in three different conformations: 1) one with high affinity for ATPγS, 2) one with low affinity, and 3) one that cannot bind ATPγS.

PAN stimulates proteolysis and gate-opening better in the 2-bound than the 4-bound states

Since PAN can exist in two different ATPγS-bound states, and ATPγS binding stimulates PAN-20S association and gate-opening, we tested whether these functions differ in the 2-bound and 4-bound states. Since the stimulation of LFP hydrolysis requires PAN-20S association and gate-opening, we examined how the rate of LFP hydrolysis was affected over a large range of ATPγS concentration. At low concentrations where PAN is in the 2-bound state (compare Fig3A to B), PAN maximally stimulated LFP degradation. Surprisingly, at higher ATPγS concentrations where PAN is in the 4-bound state, the rate of LFP degradation decreased by about 25%. When a similar experiment was carried out with ^{14}C-casein as the substrate, similar results were obtained (Fig 3C). In the 2-bound state, casein degradation was maximal, but in the 4-bound state PAN's ability to activate casein degradation was diminished by about 20%. Therefore, PAN's ability to catalyze the degradation of peptides and unfolded proteins was maximal with 2-ATPγS bound, but these activities are reduced when PAN binds two additional ATPγS's molecules.

The 2-bound state has a higher affinity for the 20S than the 4-bound state

This fall in PAN's activity in the 4-bound state could be due to a decrease in PAN's affinity for the 20S or in the ability to cause gate-opening. To determine if PAN's affinity for the 20S differed in the 2-bound and 4-bound states, we used Surface Plasmon Resonance (SPR) to monitor its affinity for the 20S. We attached the 20S proteasome to the surface of the SPR chip via its β-His tag and flowed PAN over the 20S without any nucleotide present or with ATPγS at two concentrations which correspond to the 2-bound or 4-bound states. In the 2-bound state, PAN's affinity for the 20S was maximal, but in the 4-bound state, its affinity was reduced by about 25% (Fig 3D). Therefore, the falloff in PAN's ability to stimulate the degradation of peptide and protein substrates in the 4-bound state correlates well with and probably results from the decrease in its association with the 20S proteasome.

Binding of protein substrates to PAN depends on ATP

Since PAN's abilities to associate with the 20S and stimulate gate-opening were both greater in the 2-bound than the 4-bound state, we investigated if PAN's other functions in protein degradation also differed in these two conformations. Because protein unfolding by PAN requires ATP hydrolysis, this function cannot be studied with ATPγS. However, the binding of protein substrates to PAN, which stimulates its ATPase activity (Smith et al., 2005 Benaroudj et al., 2003), must precede unfolding and degradation and may also require bound ATP. To test if protein substrates have a higher affinity for PAN in the ATP-bound state than in the ADP-bound state, we developed a method to monitor protein binding to PAN using fluorescence polarization with FITC-tagged casein or GFP-ssrA.

We used fluorescent polarization to detect such changes in FITC-casein and GFP-ssrA association with PAN. Although ADP did not cause a polarization of FITC-casein, ATP (1 mM) caused a small but highly reproducible 7 mP change in polarization (Fig 4A). When ATPγS (1 mM) was added, a much larger (56 mP) change in polarization was observed. Presumably, this effect of ATP was small due to its rapid hydrolysis to ADP. Therefore, the binding of ATPγS, and presumably ATP, to PAN stimulates the association of FITC-casein with PAN. In similar fluorescence polarization experiments with GFP-ssrA as the ligand, we found that ADP also had no effect, but ATPγS markedly stimulated polarization of GFP-ssrA (Fig 4A) as well as of a fluorescamine-conjugated ssrA peptide, (but not a ssrA-variant incapable of binding (not shown). (Because PAN + ATP unfolds GFP-ssrA, we could not assay binding with ATP present.)

Substrate binding is greater in the 2-bound than in the 4-bound state

Because substrate association with PAN is dependent on nucleotide binding, we tested if this function of PAN also differed in the 2- and 4-bound states by comparing the change in polarization of FITC-casein (0.1 μM) or GFP (0.09 μM) at different concentrations of ATPγS. Low ATPγS concentrations (i.e. the 2-bound state) supported maximal FITC-casein (Fig 4C) and GFP-ssrA (Fig 4D) association with PAN, but at higher concentrations (i.e. the 4-bound state) binding of both substrates was diminished. These curves thus resemble closely our earlier observations on other PAN functions (i.e. stimulation of peptide and protein hydrolysis and 20S association).

Unfortunately, in these fluorescence polarization assays, PAN had to be used at a concentration of 6μM PAN monomer (which is much greater than its Kd for ATPγS) and was therefore done under ligand depletion conditions, which shifts the binding curve to the right. Nevertheless, these results also clearly show a biphasic binding curve for these two substrates, further indicating reduced functional capacity when four nucleotides are bound.

With 2ATP and 2ADP bound, PAN functions similarly to the 2-bound state

Together, these experiments indicate that PAN functions optimally in the 2-bound state and suboptimally with four ATPγS bound. One possible explanation of this behaviour is that the 2 low affinity sites function normally as ADP-binding sites, but at high ATPγS concentrations, this ATP analog binds to these ADP sites (but with lower affinity). Thus, in the 4-bound state, ATPγS binding to the ADP sites may induce an unnatural conformation in the ATPase ring. We therefore determined if PAN could bind ATPγS and ADP in a mixed state, and what were the functional consequences of simultaneously binding 2 ATPγS and 2 ADPs. We initially saturated PAN with ^{14}C-ADP (100μM) and determined how many ADP molecules were bound to PAN. As found with ATP and ATPγS, PAN bound four ADPs even at saturating concentrations (Fig 5A). After incubation with ^{14}C-ADP, we added 50 μM nonradioactive ATPγS, which when ADP is not present, results in 2-ATPγS molecules binding to PAN (Fig 3). After the addition of 50 μM ATPγS to PAN that was saturated with ^{14}C-ADP, exactly 2 molecules of ADP were displaced from PAN. Since the binding of 2 molecules of ATPγS is required to displace 2 ADP molecules, PAN must simultaneously bind 2 molecules of ADP and 2 molecules of ATPγS.

In addition, we monitored the dissociation of the fluorescent analog of ADP, mant-ADP (m-ADP), in real time starting with saturating concentrations of m-ADP (50μM). When PAN binds m-ADP its fluorescence increases, and adding saturating concentrations of other nucleotides can prevent the re-binding of dissociated m-ADPs to PAN. When 50mM ATPγS was added, approximately 50% of the ADP dissociated as was expected based on the results in Fig 5 and Fig S2A. When 1mM ATPγS was added, the m-ADP fluorescence decreased to basal levels, and adding an additional 1mM ADP (with the ATPγS present) had no further effect, suggesting that all the pre-bound m-ADP had been displaced from PAN. Thus, the 4 prebound ADPs can be completely displaced from PAN when the 2 high and 2 low affinity ATP sites are occupied with ATPγS.

To determine if the 2 ADP-2 ATPγS state functions like the 2-bound or the 4-bound state and to confirm that 2 ATPγS were bound in this mixed state, we assayed PAN's ability to stimulate gate-opening. Whether PAN was in the 2-bound (i.e. 50μM ATPγS) or the 2 ATPγS + 2 ADP state (i.e. 50μM ATPγS + 100 μM ADP), it stimulated gate-opening (LFP hydrolysis) to the same extent (Fig 5b). This result confirms that 2 ATPγS replaced 2 ADP, since 2 ADPs were released, and ATPγS binding is required to stimulate LFP degradation. Thus, PAN appears to function optimally, either with 2 molecules of ATPγS bound or with 2

molecules of ATPγS and 2 of ADP bound. Presumably, this condition mimics the active state in vivo or in vitro when ATP is being hydrolyzed to ADP.

ADP dissociation is the rate limiting step in ATP hydrolysis

PAN appears to be most active with two ATPs and two ADPs bound in the steady state, but what might trigger the binding of new ATPs after ATP hydrolysis occurs? Presumably, since no more than 4 nucleotides can ever bind to the hexamer, the empty subunits cannot bind new ATPs until 2 ADPs have left. To test this hypothesis, we measured the off rate of ADP in real time using m-ADP. 5uM PAN was incubated with 25 μM m-ADP (i.e. enough to generate near-maximal fluorescence, data not shown) followed by addition of saturating ADP (2mM) or ATPγS (2mM) (Fig S2B&C). A rapid decrease in the fluorescence of m-ADP was observed that fit to an exponential decay curve. The off-rate in the presence of ADP was estimated to be 0.24 +/−0.05 (sec^{-1}), and thus the 4 ADP on PAN have a bound half-life of 3 +/− 0.6 seconds (Fig s2C). The ADP off-rate in the presence of ATP was similar with a dissociation constant of 0.26 +/−0.06(sec^{-1}), or a bound half-life of 2.7 +/− 0.6 sec. When the m-ADP dissociation curves with ATP and ADP were overlaid on the same graph (Fig S2D), it was clear that ATP and ADP caused similar rates of m-ADP release. Therefore, ATP hydrolysis does not appear to accelerate the leaving of ADP and by extension must not promote the binding of new ATPs. Since PAN in the ADP-saturated state has 4 ADPs bound, and it takes ~3 seconds for two (50%) of them to leave, this implies that an ADP molecule dissociates every 1.5 +/− 0.6 seconds. Since the rate of ADP dissociation is equivalent to the rate of ATP hydrolysis (~1/second at 37°C), it is likely that ADP dissociation is the rate-limiting step in ATP binding and hydrolysis.

Like PAN, the 26S proteasome exhibits high and low affinity binding sites for *ATPγS*

Because many insights about the role of ATP in the functioning of the PAN-20S complex apply to the eukaryotic 26S proteasome (Smith et al., 2005; Smith et al., 2007; Zhang et al., 2009a; Zhang et al., 2009b), we tested if the 26S ATPases display a similar multiphasic dependence on nucleotide concentration. Because 26S particles are heterogeneous and include singly and doubly capped populations, the number of bound nucleotides could not be determined accurately. Instead, we monitored the degradation rate of different fluorogenic substrates at different ATPγS concentrations to determine whether gate-opening by the 26S ATPases is more efficient at low than at high concentrations. 26S proteasomes purified from bovine liver or yeast were studied, and the hydrolysis of suc-LLVY-amc and suc-GGL-amc used to monitor gate-opening. Two clear phases were observed, a maximal activation at low concentrations and a reduced activation at higher concentrations (Fig. 5 C&D), exactly as was found with the PAN-20S complex.

We also determined if the 26S proteasome, like PAN, preferentially bound FITC-Casein in the ATP-bound state using ATPγS and monitoring FITC polarization (Fig S1). In fact, the binding of FITC-casein to the 26S was maximal, when the high affinity ATPγS binding sites were occupied (50 μM ATPγS) and was reduced when the low affinity sites were also occupied (2mM ATPγS). Thus, the 26S ATPases also contain high and low affinity binding sites for ATPγS, whose Kd's were nearly identical to those found for PAN. Furthermore, ATP binding to the high affinity sites allows for maximal gate-opening and protein binding, while additional binding to fill the low affinity sites decreases these critical functions. Therefore, the six 19S ATPases, Rpt1–6, must bind nucleotides and activate gate-opening and protein association in a very similar fashion as does PAN. The homologous archaeal and eukaryotic ATPases thus appear to bind and hydrolyze ATP with similar allosteric mechanisms, even though one is a homohexamer and the other a heterohexamer with many associated proteins.

Discussion

Due to the structural and functional complexity of the 26S proteasome, it is difficult to deconstruct its ATP-dependent operations into simpler mechanistic steps. A full understanding of these mechanisms requires precise knowledge of how the regulatory ATPases bind and hydrolyze ATP. PAN utilizes ATP in a similar fashion to the several other AAA ATPases that have been characterized: 1) it hydrolyzes ATP slowly (~1/sec), 2) it is stimulated by substrate binding (Benaroudj et al., 2003), 3) it hydrolyzes ATP in a non-concerted manner (Fig 2), and 4) it exhibits three different types of nucleotide binding sites, even though it contains a single type of subunit (Fig 2). Therefore, we could define the functional effects of substoichiometric ATP binding to PAN in ways that would not have been possible with other AAA ATPases. The presence of different types of nucleotide binding sites in homohexameric AAA ATPase complexes has been reported previously (Hersch et al., 2005; Singleton et al., 2000; Yakamavich et al., 2008; Zalk and Shoshan-Barmatz, 2003). This binding asymmetry must originate from the binding of a nucleotide to one subunit causing conformational changes in the neighboring ones that then differ structurally from the original ATP-bound subunit. However, since these subunits are in a ring, and each has 2 neighbors, a change in the conformation of one must induce a change in one or both of its neighbors. One structural feature of AAA ATPases that has such influence is the arginine finger (Lupas and Martin, 2002), which allows one subunit to detect a bound nucleotide in its neighbor. Thus, each subunit's conformational status can continuously influence its neighbors', so that allosteric changes can perpetuate around the ring, provided the necessary energy is available from ATP binding and hydrolysis to drive these cyclical transitions. Because this cycle of conformational changes can drive the many different activities that the AAA ATPases catalyze, elucidating the common pattern of ATP turnover is critical in understanding their functions.

Nucleotides bind to PAN in pairs

PAN's subunits exhibit three different types of conformations with 2 subunits simultaneously assuming each conformation: 1) one that binds ATPγS with high affinity, 2) one that binds ATPγS with low affinity (presumably the sites normally containing ADP), and 3) one that fails to bind any nucleotide. In addition, the binding of the first 2 ATPγS molecules to the high affinity sites is cooperative (h=1.6) as is the binding to the low affinity sites (h=2.4). Thus, binding of the first ATPγS to a subunit allosterically alters another subunit that promotes the binding of the second ATPγS. The fact that PAN exhibits positive cooperativity for ATPγS for two different subunit conformational states supports two conclusions: 1) that nucleotides bind in pairs, since binding of the first ATPγS to a high affinity site promotes the binding of a second, as also occurs in occupancy of the low affinity sites, and 2) this cooperativity implies that the subunits' conformations are induced by binding of the first nucleotide and thus do not preexist in the nucleotide-free state. In addition, when four nucleotides of any kind are bound to PAN, the fifth and sixth subunits must be in a conformation that cannot bind nucleotides. Some subunit conformations therefore restrict the conformational possibilities of the neighboring subunits. Thus, these complexes appear to function with specific operational restrictions that govern the binding pattern of ATP, such that an ordered pattern of ATP hydrolysis will emerge.

While we initially utilized ATPγS instead of ATP, the 2 high affinity subunits presumably bind ATP, and the 2 low affinity ATPγS sites are the sites where ADP would be bound when generated by hydrolysis. In contrast to ATPγS, ADP binding to these low affinity sites does not reduce the enzyme's maximal activity (Fig 5). Therefore, the presence of the first 2 ATPs on PAN induces a conformational change in two other subunits that allows ADP binding, but inhibits the binding of ATP. The sensor II motif on AAA ATPases seems likely to communicate such structural transitions between neighboring subunits, since it is required

for several AAA enzymes to change their conformations upon ATP binding (Hattendorf and Lindquist, 2002;Ogura and Wilkinson, 2001). It is difficult to determine if the conformation of the empty subunits is induced by ATPγS binding to the high affinity or low affinity sites, since assaying the empty subunits requires the presence of nucleotides in both of the other conformations. However, clearly both ATP and ADP can induce this empty conformation because neither of these nucleotides can occupy more than four subunits.

ATP Hydrolysis by pairs of subunits acting in concert

Since ATP binding occurs in pairs and is cooperative for both the high and low affinity sites, ATP molecules are also most likely hydrolyzed in pairs by subunits functioning in concert. Presumably, as ATP is hydrolyzed in a single subunit, the new ADP likely induces a further conformational change in the other "paired" ATP-bound subunit promoting its hydrolysis to ADP, since nucleotide binding to the low affinity sites (ADP sites) is highly cooperative (Figure 3). Thus, not only is ATP binding a coupled event, but also ATP hydrolysis appears to be coupled. This hexameric organization and coupled behavior of paired subunits are most likely critical in the conversion of the energy from ATP hydrolysis into mechanical work. For example, if the various subunits hydrolyze ATP individually, then their force-delivering domains (e.g. pore loops that are thought to translocate substrates) are likely to function only as isolated events to "swat" at substrates. However, if two subunits hydrolyze ATP in concert and thus move together, then a more efficient mechanism can be applied to grab substrates to deliver force to drive substrate translocation and unfolding.

The cyclical arrangement of these ATPase subunits and their high degree of positive and negative allostery suggest that ATP hydrolysis occurs in a specific pattern during normal functioning, although this pattern may not be rigidly adhered to. In fact, rigid adherence to one pattern could impair the functioning of the complex, especially in instances where substrates resisted unfolding or translocation. Martin et. al. (2005) elegantly showed that the ClpX ATPase could still hydrolyze ATP (albeit at very impaired rates) even when only one of its six subunits was active. Therefore, a single subunit appears capable of sampling the ATP-bound, ADP-bound, and empty states, even in the absence of dynamic conformational influences from neighboring subunits (although their experiments cannot rule out that inherent ATP binding and dissociation from the mutated subunits did not cause the critical conformational changes). However, these findings with a single active subunit do not imply that ATP hydrolysis is normally a completely random process. For a hexameric complex to hydrolyze ATP purely stochastically, the function of each subunit must be uncoupled from the others, and there should be no subunit-subunit communication or cooperativity, which is obviously not the case for PAN and the other well-characterized AAA+ ATPases.

An ordered pattern of ATP hydrolysis

Since PAN cannot simultaneously bind nucleotides on all six of its subunits, some fundamental mechanism must govern which subunits can bind which nucleotides. If one PAN subunit binds ATP, then the conformations of its neighbors must be restricted to certain states, since no more than two subunits can simultaneously assume the high affinity state. Therefore, the conformation of one subunit must limit the possible conformations of its neighbors and their capacity to bind ATP. Three observations argue strongly that PANs subunits (and presumably other AAA family members) hydrolyze ATP in a specific pattern: 1) the complex binds ATP in pairs, 2) the subunits co-exist in three conformational states, and 3) that PAN in its maximally functional state has 2 subunits with ATP bound, 2 with ADP, and 2 lacking nucleotides (Fig. 7). There is only a finite number of ways that 2 ATP molecules can bind around a hexameric ring, and these three observed properties eliminate several possible patterns. The "binding in pairs" observation rules out a purely concerted mechanism where all subunit hydrolyze ATP simultaneously.

A pair of ATPs can only bind a hexameric ring in 3 ways: to adjacent subunits (“ortho”), to two subunits with an empty subunit in-between (“meta”), or across the ring from one another (“para”) (Figure 7A). We can distinguish between these three possibilities if we make a simple assumption—after ATP binds to a subunit, its conformation always induces the same conformational state in the adjacent subunits that differ from its own conformation —(e.g. the ATP bound subunit always causes the counterclockwise subunit to assume the ADP-bound state). Only para-binding of ATP is consistent with this simple assumption and with the finding that nucleotides bind in pairs. Both “ortho” and “meta” binding require that the ATP-bound subunits induce multiple types of conformations in the same neighbor, which would not be consistent with a complex containing 6 subunits that strictly exhibit three pairs of different conformational states. This requirement implies that one conformation always determines those of its neighbors and seems most plausible for identical subunits that cycle through ATP-driven conformational changes around a homohexameric ring.

Moreover, this initial ATP binding pattern predicts that a cyclical pattern of ATP hydrolysis is most likely to emerge (Fig 7 B). The simplest model to explain these results is that ATP binding to one subunit induces the ADP-bound state in one of its neighbors and the nucleotide-free state in the other. As a result, the following nucleotide binding-exchange model seems most likely: 1) the bound ATP is hydrolyzed to ADP with rapid release of the free phosphate (Fig 2 C), 2) the previously bound ADP in the neighboring subunit is released generating an empty site, and 3) ATP could then bind to the initially empty site. Then, the cycle would repeat. Since ADP leaving must precede the binding of a new ATP pair (because PAN cannot bind more than 2 pairs of nucleotides), ADP-release would be expected to be the rate-limiting step that allows a new ATP to bind, as we observed (Fig S2B,C, and D). Such a cycle could still function if one subunit stalls or fails to hydrolyze ATP, since ATP binding to a new empty subunit would reestablish a new pattern and allow repeated rounds of ATP hydrolysis to continue.

Several highly relevant mutations have been generated in the subunits in the para positions in bacterial ClpX ATPase by (Martin et al., 2005) and extrapolation to PAN seems justified since these AAA+ ATPases share considerable homology in their ATPase domains and subunit-subunit interfaces (i.e. in the sensor II and arginine fingers domains). Although all such mutations reduce ATPase function, para Sensor II mutations that prevent conformational changes upon ATP binding had twice as much activity as Para mutations that prevent ATP hydrolysis, but allow ATP binding and the resulting conformational changes (Martin et al., 2005). Accordingly, our model predicts that ATP binding to para subunits without hydrolysis should prevent further ATP binding to the adjacent WT subunits. In other words, allowing ATP-induced conformational changes in the para subunits actually inhibits ATP hydrolyisis in the other WT subunits (Martin et al., 2005). Furthermore, similar para mutations that are counterclockwise to the WT subunits impair ATP hydrolysis in the WT subunit (Martin et al., 2005). On this basis, it seems most likely that ATP induces an empty subunit specifically in the clockwise neighbor and an ADP-bound subunit in the counterclockwise neighbor, thus establishing a clockwise directionality for the ATPase cycle.

Further support for this nucleotide binding-change model comes from the crystal structures of other hexameric AAA+ ATPases, all of which show substoichiometric amounts of bound nucleotides (Glynn et al., 2009; Singleton et al., 2000). In fact, Singleton et. al. proposed a similar nucleotide binding model (with ATP binding subunits positioned across the ring from each other) for the T7 gene 4 ring helicase. Interestingly, this homohexamer displays a “dimer of trimers” conformational symmetry suggesting a substoicheometric nucleotide binding pattern around the ring. The crystal structure of mutated, linked ClpX also shows a

similar dimer of trimers structure (Glynn et al., 2009). While similar nucleotide exchange reactions have been suggested by others (Hersch et al., 2005; Schumacher et al., 2008; Singleton et al., 2000), although without evidence of distinct functional consequences, the crystal structures of some AAA ATPases (e.g. HslU (Bochtler et al., 2000; Sousa et al., 2000; Yakamavich et al., 2008)) revealed seemingly promiscuous binding patterns for ATP analogs or ADP. An unambiguous elucidation of the binding-exchange reactions for those ATPases has proven difficult, because the number of nucleotides bound per hexamer has rarely been determined to a definite integer value (i.e. prior results could not distinguish between 3 or 4 nucleotides per hexamer). This ambiguity has made it impossible to reach conclusions regarding their binding-exchange reactions. In contrast, here we have been able to obtain unambiguous values for the number of nucleotides bound to PAN, and to demonstrate directly that a single homohexamer can exhibit two different types of ATP binding sites. These properties have allowed us to generate a clearer nucleotide binding exchange model for the AAA ATPases than was possible previously.

Paired ATP binding implies only two ATPases C-termini dock into 20S at any time

A long-standing mystery regarding the structure and function of the 26S and the PAN-20S complex is the symmetry mismatch problem—how can the six ATPase subunits interact with and regulate the 7-subunits in the proteasome's outer ring. It is well established that the ATPases' C-termini dock into the intersubunit pockets in the α-ring to induce gate-opening (Smith et al., 2007), but the number of C-termini and number of pockets interacting at any instant are unclear. Because ATP binding induces this association of the C-terminal HbYX motif with these pockets, it is very likely that the subunits whose C-termini associate with the proteasome are those subunits with a bound ATP. Accordingly, in the homologous ATPase, HslU, ATP binding to subunits leads to exposure of the buried C-termini (Sousa et al., 2000). The present findings therefore imply strongly that at any time, only 2 of the ATPases in the hexameric ring ever associate with 20S. In fact, maximal gate-opening was observed with 2 ATPγS bound to the complex (Fig. 3A/B and Fig 7B). As discussed above, it is most likely that the ATP-binding pair lie across the ring from one another, and therefore at any instant, it is these para-positioned C-termini that dock into the 20S pockets.

If true, then the distance between PAN's para-positioned C-termini and the respective 20S intersubunit pockets must be similar. Although no information is available concerning the distances between PAN's C-termini, there is structural information about the C-termini of the homologous ATPase, HslU (whose C-termini are exposed upon ATP-binding (Sousa et al., 2000)), as well as the distances between the intersubunit pockets in archaeal 20S. Interestingly, the distance between HslU's para C-terminal carboxyl groups in the ATP bound form is 65 Å (Fig. 8C, 1G3I), while that between Lys66 in the intersubunit pockets across the 20S α-ring, with which PAN's C-termini interact (Yu et al., 2010) is 68 Å (3IPM, see figure 8C). Since the distance between the C-terminal carboxyl group and the NH_2-group of the 20S's lysine 66 is 2.5 Å, these distances are nearly ideal for the 2 para C-termini to interact with these lysines in the opposing 20S intersubunit pockets (Fig 7C).

Paired ATP binding explains wobbling of the ATPases ring on the 20S

This conclusion leads to two key predictions that can account for prior observations on the structures of archaeal and eukaryotic ATPase-20S complexes: 1) that the central axes of the ATPase and the 20S cannot be aligned due to the symmetry mismatch of the rings, and 2) that the ATPase rings can have only limited and dynamic contacts with the 20S. As ATP is hydrolyzed, new pairs of para subunits must bind ATP and their C-termini associate with different pockets in the α-ring allowing the ATPase ring to "wobble" on top of the 20S. Electron micrographic evidence for "wobbling" of the ATPases on the 20S has been presented for PAN (Smith et al., 2005) and the 26S proteasome (Walz et al., 1998).

Recently, Baumeister's group showed that in the 26S, the 19S base is also positioned off axis relative to the 20S proteasome (Nickell et al., 2009), and upon careful inspection of our prior EM images (Smith et al., 2005), we found that PAN is also situated off the 7-fold axis of the 20S. Therefore, both predictions based on the para-position binding of ATP and the para C-terminal interactions, are consistent with the structures of the PAN-20S and 26S complexes.

Suboptimal function of the 4-bound state may result from steric hindrance of the ATPase-20S interaction

The surprising finding that PAN with 2 ATPγS bound had a higher affinity for the 20S than with 4 ATPγS (Fig 3) suggests that the number and arrangement of PAN's C-termini that dock into the 20S are critical in determining this affinity. Thus, when 2 ATPγS are bound, presumably in the para positions PAN's affinity for the 20S is strongest. However, when four ATPγS are bound, and four C-termini are available for 20S interactions, the affinity is reduced. Interestingly, as shown in Fig 7C right, the structural arrangement of PAN's four C-termini is less compatible sterically with docking into the 20S's 7 pockets than the binding of only 2 para-C-termini. These steric considerations for the PAN-20S interactions should also apply to the eukaryotic 26S because of their close structural homologies (Zhang et. al. 2009a) and in both cases can explain the reduction in gate-opening in the 4-bound state.

Implications for functioning of the heteromeric 26S ATPase ring

In the 26S, gate-opening and binding of the unfolded polypeptide, FITC-Casein, show very similar biphasic dependence on ATPγS as we found for the PAN-20S complex, and in both, these activities were maximal only when the high affinity sites were occupied. Like PAN and the 20S, the eukaryotic 19S and 20S associate when ATP is present and dissociate in its absence, but the association and dissociation kinetics are much slower for the 26S complex (Liu et al., 2006; Smith et al., 2005). Possibly, there are inherent differences between the ways that the 19S ATPases (Rpt1–6) and PAN associate with the 20S. PAN's six identical C-termini share two roles: to induce gate-opening and to promote association with the 20S. By contrast, the different 19S C-termini seem to perform only one of these two roles. Only Rpts 2, 3, and 5 contain the gate-opening HbYX motif, and mutations in them cause gating defects, but do not reduce 26S stability (Smith et. al. 2007). However, the non-HbYX C-termini, Rpt 1, 4, and 6, are required for the 19S–20S interaction and thus 26S assembly (Park et al., 2009; Smith et al., 2007). Thus, the C-termini of the non-HbYX containing Rpts may be specialized to provide greater stability for the complex. The 19S also contains additional subunits that may stabilize the 19S–20S interaction (Bohn et al., 2010; da Fonseca and Morris, 2008; Kleijnen et al., 2007; Leggett et al., 2002).

Recent crosslinking studies unambiguously confirmed the order of the 26S ATPases to be Rpt1-2-6-3-4-5 (Tomko et al., 2010). This ordering of subunits produces an intriguing pattern in which the HbYX-containing (Rpts 2, 3, and 5) and non-HbYX (Rpts 1, 4, and 6) subunits alternate (Fig. 7). Therefore, according to the para binding model, ATP would always bind to one HbYX subunit and one non-HbYX subunit (Fig 7A). Consequently, one "gate-opening" HbYX C-terminus and one "high affinity" non-HbYX C-termini would be engaged with the 20S in all possible ATP bound patterns. Therefore, in addition to accounting for the symmetry mismatch, this model with only 2 para-subunits binding ATP and docking into the α–ring at any one time could allow the hexameric ATPase to hydrolyze ATP cyclically and to drive protein unfolding while remaining associated with the 20S and opening its gate. This model thus integrates and can account for multiple features of the proteasome. Specifically, it explains how, despite the symmetry mismatch, rounds of ATP binding and hydrolysis occur and allow continuous association of the ATPases with the

proteasome and opening of its gate for substrate entry while causing conformational changes in the rest of the ATPase molecule that drive substrate unfolding and translocation into the 20S for degradation.

EXPERIMENTAL PROCEDURES

Materials, Protein Expression and Purification

PAN, GFPssrA, *Thermoplasma* 20S (T20S), rabbit muscle 26S (R26S), LFP (Mca-AKVYPYPME-Dpa[Dnp]-amide) and [^{14}C]methyl-casein were prepared as described (Smith et al., 2007). Yeast 26S (Y26S) proteasomes were isolated using the Ubl affinity purification described by Besche et. al. (Besche et al., 2009). ATP (99%), ATPγS (95%), and ADP (99%) were purchased from Sigma and were stored at −80°C until use. FITC-casein (Sigma) was dissolved in Hepes (50 mM, pH 7.5) and loaded onto a P10 column (Amersham) to remove residual free FITC. ssrA and ddssrA peptides were synthesized at Tufts core facility, (Boston, MA) and were dissolved in 50mM Hepes (pH 7.5). Peptide concentration was determined by the absorbance at 280 nm. For polarization studies, peptides were reacted with a 100 fold excess of fluorescamine (Sigma) in amine-free buffer and were used within 2hrs of labeling.

ATPase Activity, 20S Gate Opening and Protein Degradation

Unless indicated otherwise, reactions with archaeal proteasomes were performed at 45°C, yeast proteasomes at 30°C, and mammalian proteasomes at 37°C. Hydrolysis of ATP was assayed by following the production of inorganic phosphate (Ames, 1966). To measure 20S gate-opening as described previously (Smith et al., 2005) fluorogenic peptide substrates (dissolved in DMSO) were used at final concentrations of 100μM for Suc-LLVY-AMC (Mammalian 20S), 20μM for Suc-GGL-AMC (yeast 20S) and 10uM for LFP (Thermoplasma 20S). [^{14}C]methyl-casein degradation was measured as described in (Smith et al., 2005) and (Benaroudj et al., 2003).

Substrate Binding

Substrate binding to PAN was monitored by fluorescence polarization. Binding of FITC-casein was measured as described (Bosl et al., 2005). PAN was added to FITC-casein at the indicated concentrations in the presence of 1mM ADP, ATP or ATPγS, 10mM MgCl2, 50mM Tris (pH 7.5). After 20 min (once maximal binding was obtained), fluorescence polarization was measured in a Spectramax Fluorstar M5 plate reader (494 nm excitation; 515nm emission). For the 26S proteasome FITC-Casein binding was measured in a micro-cuvette on a Varian Carry Eclipse Fluorometer (4nM Bovine liver 26S and 4nM FITC-Casein) with the indicated concentrations of ATPγS and 10μM MG132 to prevent degradation. GFPssra polarization was measured as described (Park and Raines, 2004) using 390 nm (excitation) and 595 nm (emission) wavelengths.

Nucleotide Binding

To determine the number of nucleotides bound to PAN, α-^{32}P ATP (MPBio, 25 Ci/mmol) was incubated with PAN (0.4mg/ml) at room temperature. PAN and the bound nucleotide were separated from the free nucleotide by centrifugation through a Sephadex G50 column as described by (Menon and Goldberg, 1987). The recovery of PAN was estimated by assaying its ability to stimulate LFP degradation by T20S, as described (Horwitz et al., 2007) and by the Bradford assay. To identify the nucleotide present in the protein fraction, 2 μl of the eluate was spotted on a silica TLC plate (Silica gel with 254 nm fluorescent indicator, FLUKA) and resolved using a mixture of dioxane:NH_4OH:H_2O (6:2:9) (Fontes et al., 2008). The position of ATP and ADP was determined by fluorescence and

phosphoimaging of the TLC plates. ATPγ^{35}S binding to PAN was measured as described (Horwitz et al., 2007). The number of ADP molecules bound per PAN hexamer was measured using ^{14}C-ADP (Amersham, 60mCi/mmol) at 500μM. Protein recovery was estimated using the Bradford assay.

Mant-ADP binding was monitored by following fluorescence at ex 365/em 445 on a Varian Carry Eclipse in a microcuvette. The reaction was run at 37°C in 50mM Tris with 1mM Dtt, 10mM MgCl, 5% glycerol, and 5μM PAN with the indicated concentrations of nucleotides. Fluorescence was monitored and the data collected in real-time. The addition of competing nucleotides and mixing required 1–2 seconds. The raw data was fit to a standard double exponential decay curve using sigma plot.

Surface Plasmon Resonance

The formation of the PAN-20S complex was monitored by Surface Plasmon Resonance with Biacore 2000 apparatus (BIAcore AB, Sweden). His-tagged 20S was immobilized on the Ni^{2+} - nitrilotriacetic acid (NTA) chip. First 10μl of 500μM $NiCl_2$ in eluent buffer (0.01M Hepes, 0.15M NaCl, 50 μM EDTA, 0.005% surfactant P20, pH 7.4) was injected onto the surface. Then 80–120 μl of 12 nM 20S in eluent buffer containing 20 mM imidazole was injected for 8–12 min (flow rate 10 μL/min). After immobilization, the buffer was changed to buffer A (50 mM Hepes, pH 7.5, with 1mM DTT, 5mM $MgCl_2$, 50 μM EDTA and 20 mM imidazole). To monitor the nucleotide requirement for the binding of PAN to 20S, PAN in the presence or absence of the indicated nucleotide concentration was injected for 150 sec at flow rate of 30 μL/min at 20 °C. The surface was regenerated between experiments by injection of 0.35M EDTA, pH 8.3. The data analysis was carried out using the BIAevaluation 2.0 software

Supplementary Material

Refer to Web version on PubMed Central for supplementary material.

Acknowledgments

This studies were supported by a grant from the NIH (GM051923-09) to A.G., the Multiple Myeloma Foundation to A.G. and by a fellowship (SFRH/26490/2006) from Fundação para a Ciência e Tecnologia, Lisboa, Portugal to H.F.

References

Ames BN. Assay of inorganic Phosphate, Total Phosphate and Phosphatases. Met in Enzym. 1966; 8:115–118.

Augustin S, Gerdes F, Lee S, Tsai FT, Langer T, Tatsuta T. An intersubunit signaling network coordinates ATP hydrolysis by m-AAA proteases. Mol Cell. 2009; 35:574–585. [PubMed: 19748354]

Benaroudj N, Goldberg AL. PAN, the Proteasome Activating Nucleotidase from archaebacteria, is a molecular chaperone which unfolds protein substrate. Nature Cell Biol. 2000; 2:833–839. [PubMed: 11056539]

Benaroudj N, Zwickl P, Seemuller E, Baumeister W, Goldberg AL. ATP hydrolysis by the proteasome regulatory complex PAN serves multiple functions in protein degradation. Mol Cell. 2003; 11:69–78. [PubMed: 12535522]

Besche H, Haas W, Gygi S, Goldberg A. Isolation of mammalian 26S proteasomes and p97/VCP complexes using the ubiquitin-like domain from HHR23B reveals novel proteasome-associated proteins. Biochemistry. 2009

Bochtler M, Hartmann C, Song HK, Bourenkov GP, Bartunik HD, Huber R. The structures of HsIU and the ATP-dependent protease HsIU-HsIV. Nature. 2000; 403:800–805. [PubMed: 10693812]

Bohn S, Beck F, Sakata E, Walzthoeni T, Beck M, Aebersold R, Forster F, Baumeister W, Nickell S. Structure of the 26S proteasome from Schizosaccharomyces pombe at subnanometer resolution. Proc Natl Acad Sci U S A. 2010; 107:20992–20997. [PubMed: 21098295]

Bosl B, Grimminger V, Walter S. Substrate binding to the molecular chaperone Hsp104 and its regulation by nucleotides. Journal of Biological Chemistry. 2005; 280:38170–38176. [PubMed: 16135516]

Briggs LC, Baldwin GS, Miyata N, Kondo H, Zhang X, Freemont PS. Analysis of nucleotide binding to P97 reveals the properties of a tandem AAA hexameric ATPase. Journal of Biological Chemistry. 2008; 283:13745–13752. [PubMed: 18332143]

da Fonseca PC, Morris EP. Structure of the human 26S proteasome: subunit radial displacements open the gate into the proteolytic core. Journal of Biological Chemistry. 2008; 283:23305–23314. [PubMed: 18534977]

Djuranovic S, Hartmann MD, Habeck M, Ursinus A, Zwickl P, Martin J, Lupas AN, Zeth K. Structure and activity of the N-terminal substrate recognition domains in proteasomal ATPases. Mol Cell. 2009; 34:580–590. [PubMed: 19481487]

Fontes R, Fernandes D, Peralta F, Fraga H, Maio I, Esteves da Silva JC. Pyrophosphate and tripolyphosphate affect firefly luciferase luminescence because they act as substrates and not as allosteric effectors. FEBS J. 2008; 275:1500–1509. [PubMed: 18279384]

Glickman MH, Ciechanover A. The ubiquitin-proteasome proteolytic pathway: destruction for the sake of construction. Physiol Rev. 2002; 82:373–428. [PubMed: 11917093]

Glynn SE, Martin A, Nager AR, Baker TA, Sauer RT. Structures of asymmetric ClpX hexamers reveal nucleotide-dependent motions in a AAA+ protein-unfolding machine. Cell. 2009; 139:744–756. [PubMed: 19914167]

Goldberg AL. Nobel committee tags ubiquitin for distinction. Neuron. 2005; 45:339–344. [PubMed: 15694320]

Groll M, Ditzel L, Lowe J, Stock D, Bochtler M, Bartunik HD, Huber R. Structure Of 20s Proteasome From Yeast At 2.4-Angstrom Resolution. Nature. 1997; 386:463–471. [PubMed: 9087403]

Hattendorf DA, Lindquist SL. Analysis of the AAA sensor-2 motif in the C-terminal ATPase domain of Hsp104 with a site-specific fluorescent probe of nucleotide binding. Proc Natl Acad Sci U S A. 2002; 99:2732–2737. [PubMed: 11867765]

Hersch GL, Burton RE, Bolon DN, Baker TA, Sauer RT. Asymmetric interactions of ATP with the AAA+ ClpX6 unfoldase: allosteric control of a protein machine. Cell. 2005; 121:1017–1027. [PubMed: 15989952]

Horwitz AA, Navon A, Groll M, Smith DM, Reis C, Goldberg AL. ATP-induced structural transitions in PAN, the proteasome-regulatory ATPase complex in Archaea. Journal of Biological Chemistry. 2007; 282:22921–22929. [PubMed: 17553803]

Kleijnen MF, Roelofs J, Park S, Hathaway NA, Glickman M, King RW, Finley D. Stability of the proteasome can be regulated allosterically through engagement of its proteolytic active sites. Nat Struct Mol Biol. 2007; 14:1180–1188. [PubMed: 18026118]

Leggett DS, Hanna J, Borodovsky A, Crosas B, Schmidt M, Baker RT, Walz T, Ploegh H, Finley D. Multiple associated proteins regulate proteasome structure and function. Mol Cell. 2002; 10:495–507. [PubMed: 12408819]

Liu CW, Li X, Thompson D, Wooding K, Chang TL, Tang Z, Yu H, Thomas PJ, DeMartino GN. ATP binding and ATP hydrolysis play distinct roles in the function of 26S proteasome. Mol Cell. 2006; 24:39–50. [PubMed: 17018291]

Lowe J, Stock D, Jap B, Zwickl P, Baumeister W, Huber R. Crystal structure of the 20S proteasome from the archaeon T. acidophilum at 3.4 A resolution. Science. 1995; 268:533–539. [PubMed: 7725097]

Lupas AN, Martin J. AAA proteins. Curr Opin Struct Biol. 2002; 12:746–753. [PubMed: 12504679]

Martin A, Baker TA, Sauer RT. Rebuilt AAA + motors reveal operating principles for ATP-fuelled machines. Nature. 2005; 437:1115–1120. [PubMed: 16237435]

Menon AS, Goldberg AL. Binding of Nucleotides to the ATP-dependent Protease La from *Escherichia coli*. J Biol Chem. 1987; 262:14921–14928. [PubMed: 3312196]

Nickell S, Beck F, Scheres SH, Korinek A, Forster F, Lasker K, Mihalache O, Sun N, Nagy I, Sali A, et al. Insights into the molecular architecture of the 26S proteasome. Proc Natl Acad Sci U S A. 2009; 106:11943–11947. [PubMed: 19581588]

Ogura T, Wilkinson AJ. AAA+ superfamily ATPases: common structure--diverse function. Genes Cells. 2001; 6:575–597. [PubMed: 11473577]

Park S, Roelofs J, Kim W, Robert J, Schmidt M, Gygi SP, Finley D. Hexameric assembly of the proteasomal ATPases is templated through their C termini. Nature. 2009; 459:866–870. [PubMed: 19412160]

Park SH, Raines RT. Fluorescence polarization assay to quantify protein-protein interactions. Methods Mol Biol. 2004; 261:161–166. [PubMed: 15064456]

Rabl J, Smith DM, Yu Y, Chang SC, Goldberg AL, Cheng Y. Mechanism of gate opening in the 20S proteasome by the proteasomal ATPases. Mol Cell. 2008; 30:360–368. [PubMed: 18471981]

Schumacher J, Joly N, Claeys-Bouuaert IL, Aziz SA, Rappas M, Zhang X, Buck M. Mechanism of homotropic control to coordinate hydrolysis in a hexameric AAA+ ring ATPase. J Mol Biol. 2008; 381:1–12. [PubMed: 18599077]

Singleton MR, Sawaya MR, Ellenberger T, Wigley DB. Crystal structure of T7 gene 4 ring helicase indicates a mechanism for sequential hydrolysis of nucleotides. Cell. 2000; 101:589–600. [PubMed: 10892646]

Smith DM, Benaroudj N, Goldberg A. Proteasomes and their associated ATPases: a destructive combination. Journal of Structural Biology. 2006; 156:72–83. [PubMed: 16919475]

Smith DM, Chang SC, Park S, Finley D, Cheng Y, Goldberg AL. Docking of the proteasomal ATPases' carboxyl termini in the 20S proteasome's alpha ring opens the gate for substrate entry. Mol Cell. 2007; 27:731–744. [PubMed: 17803938]

Smith DM, Kafri G, Cheng Y, Ng D, Walz T, Goldberg AL. ATP binding to PAN or the 26S ATPases causes association with the 20S proteasome, gate opening, and translocation of unfolded proteins. Mol Cell. 2005; 20:687–698. [PubMed: 16337593]

Sousa MC, Trame CB, Tsuruta H, Wilbanks SM, Reddy VS, McKay DB. Crystal and solution structures of an HslUV protease-chaperone complex. Cell. 2000; 103:633–643. [PubMed: 11106733]

Tomko RJ Jr, Funakoshi M, Schneider K, Wang J, Hochstrasser M. Heterohexameric ring arrangement of the eukaryotic proteasomal ATPases: implications for proteasome structure and assembly. Mol Cell. 2010; 38:393–403. [PubMed: 20471945]

Walz J, Erdmann A, Kania M, Typke D, Koster AJ, Baumeister W. 26S proteasome structure revealed by three-dimensional electron microscopy. Journal of Structural Biology. 1998; 121:19–29. [PubMed: 9573617]

Yakamavich JA, Baker TA, Sauer RT. Asymmetric nucleotide transactions of the HslUV protease. J Mol Biol. 2008; 380:946–957. [PubMed: 18582897]

Yu Y, Smith DM, Kim HM, Rodriguez V, Goldberg AL, Cheng Y. Interactions of PAN's C-termini with archaeal 20S proteasome and implications for the eukaryotic proteasome-ATPase interactions. Embo J. 2010; 29:692–702. [PubMed: 20019667]

Zalk R, Shoshan-Barmatz V. ATP-binding sites in brain p97/VCP (valosin-containing protein), a multifunctional AAA ATPase. Biochem J. 2003; 374:473–480. [PubMed: 12747802]

Zhang F, Hu M, Tian G, Zhang P, Finley D, Jeffrey PD, Shi Y. Structural insights into the regulatory particle of the proteasome from Methanocaldococcus jannaschii. Mol Cell. 2009a; 34:473–484. [PubMed: 19481527]

Zhang F, Wu Z, Zhang P, Tian G, Finley D, Shi Y. Mechanism of substrate unfolding and translocation by the regulatory particle of the proteasome from Methanocaldococcus jannaschii. Mol Cell. 2009b; 34:485–496. [PubMed: 19481528]

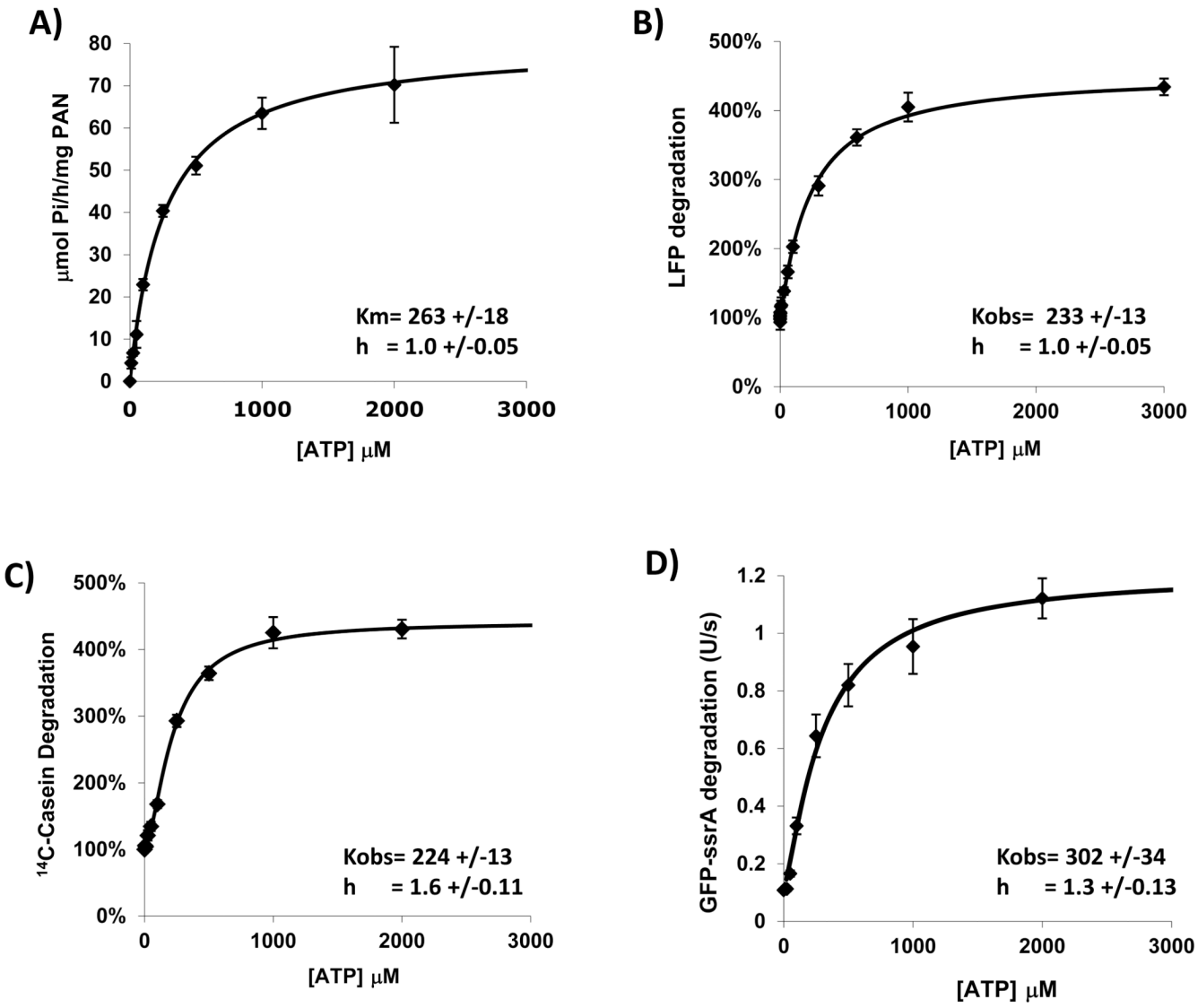

Figure 1. Effect of increasing ATP concentration on PAN's ability to hydrolyze ATP and to stimulate degradation of three different types of substrates

A) The rate of ATP hydrolysis by PAN at different ATP concentrations. All data are the means of three or more independent experiments +/− SD.

B) The degradation rate of the fluorogenic octapeptide (LFP) by the PAN-20S complex. The activity without added nucleotide is taken as 100% for B and C.

C) The degradation rate of ^{14}C-casein to acid-soluble peptides by the PAN-20S complex.

D) The degradation rate of GFP-ssrA (monitored by loss of fluorescence) by the PAN-20S complex. Since PAN alone can unfold GFP, 20S was added in excess to ensure that unfolding was coupled to degradation.

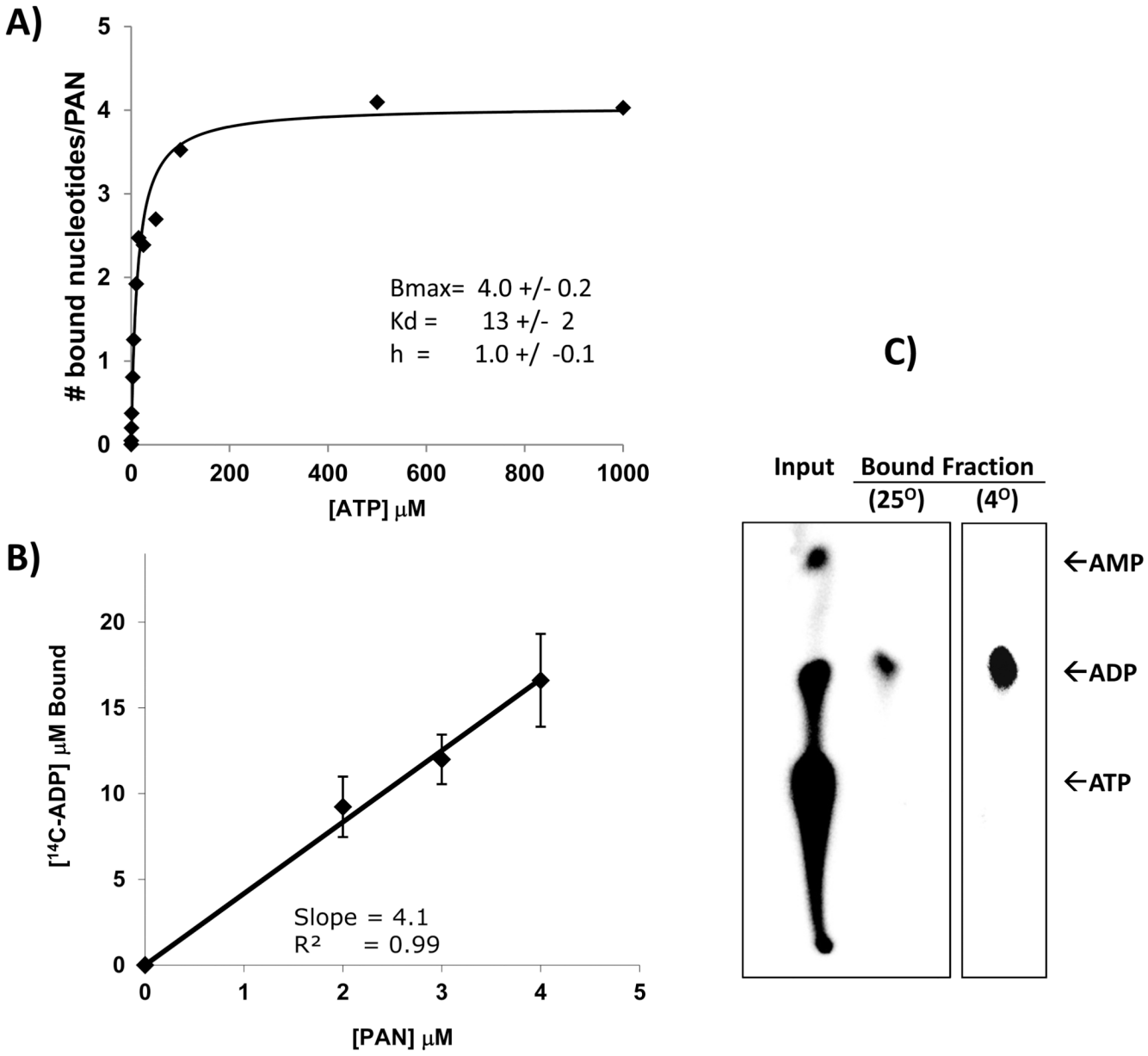

Figure 2. PAN can bind up to 4 nucleotides per hexamer and hydrolyzes ATP even at 4°C

A) The number of bound α-^{32}P-ATP to PAN hexamer (0.4mg/ml) was determined at different ATP concentrations at 4°C, following isolation of the nucleotide bound complex by rapid spin through a size exclusion column. The data in A and B are the means of three independent experiments +/− SD.

B) The concentration of ^{14}C-ADP that was bound to PAN with increasing concentrations of PAN using saturating ^{14}C-ADP (1 mM).

C) Bound ATP is rapidly hydrolyzed to ADP. α-^{32}P-ATP was incubated with PAN at 4° or 25° C and the bound nucleotides were isolated into a reaction-quenching buffer, and analyzed on silica TLC plate. The image is representative of 3 independent experiments. Identical experiments using γ^{32}P-ATP showed that the hydrolyzed Pi was released from PAN.

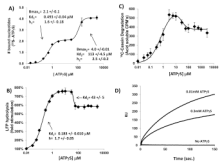

Figure 3. PAN contains two different types of binding sites for ATPγS and its ability to associate with the 20S and open its gate are greater with 2 ATPγS bound than with 4 bound

A) The number of ATPγS molecules bound to PAN was determined at different ^{35}S-ATPγS concentrations at 25°C, following isolation of the complex as in Fig 2A. The data from A, B and C are the means of three independent experiments +/− SD.

B) The rate of LFP hydrolysis (a measure of gate-opening) by the PAN-20S at different ATPγS concentrations.

C) The rate of ^{14}C-casein degradation to acid soluble peptides by the PAN-20S complex at different ATPγS concentrations.

D) The association of PAN with the 20S proteasome, as determined by surface plasmon resonance, is greater at low ATPγS concentrations (0.01 mM) where 2 ATPγS are bound than at high concentrations (0.3mM) where 4 are bound. These curves are representative of more than 3 independent experiments.

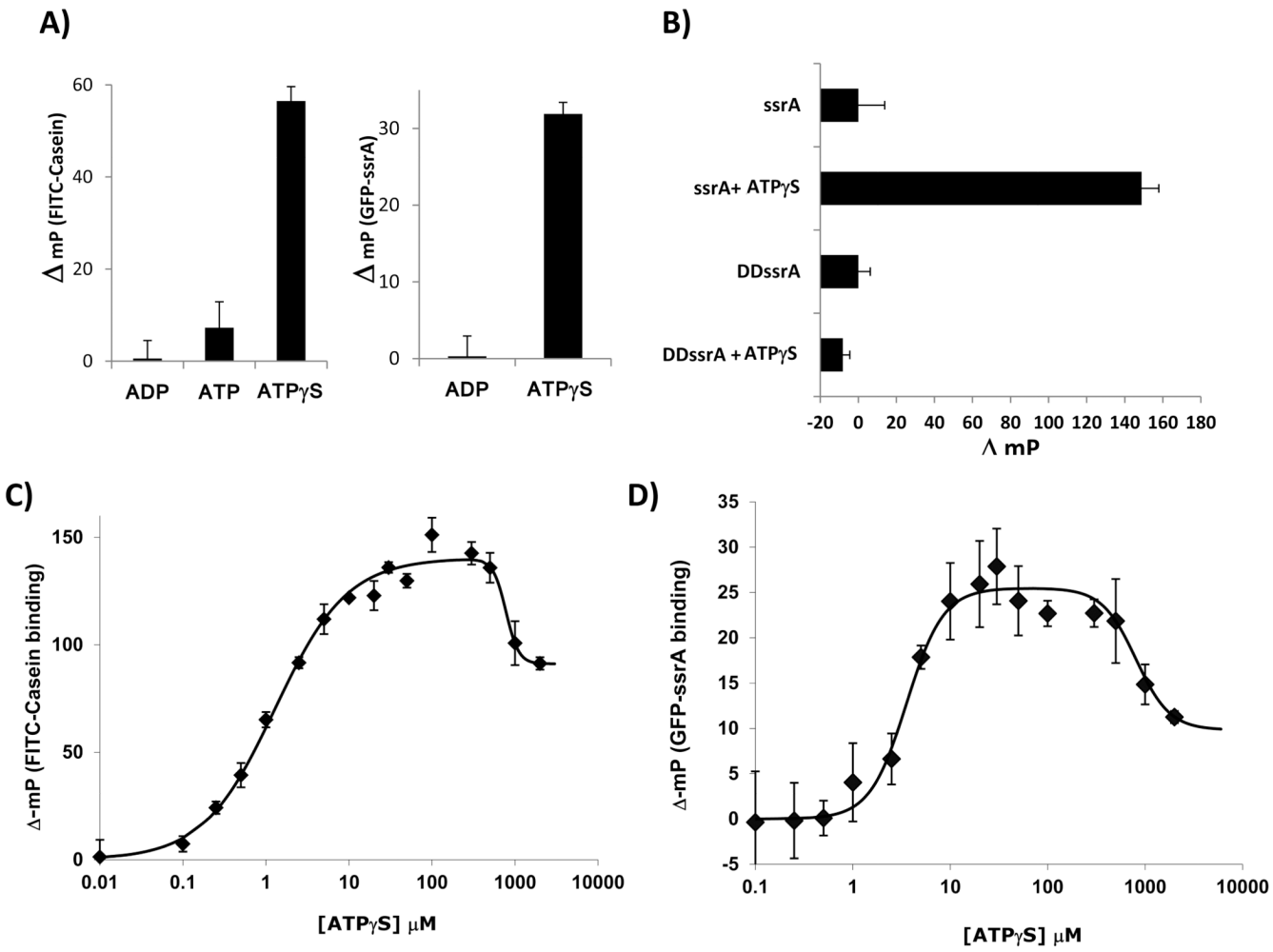

Figure 4. ATP binding to PAN stimulates binding of protein substrates

A) Binding of FITC-casein (0.1 μM) or GFP-ssrA (0.08 μM) to PAN was monitored by fluorescence polarization in the presence of different nucleotides (1mM).

B) PAN's ability to bind a fluorescamine-labeled-ssrA peptide (0.5μM; ANDENYALAA) or an ssrA peptide with two aspartates in its C-terminus, DDssrA, (ANDENYALDD) was determined in the presence or absence of ATPγS (0.1mM).

C) The change in polarization of FITC-casein (0.1 μM) by PAN at different ATPγS concentrations. Due to the high level of fluorescence intensity required for polarization assays, PAN had to be used at 1 μM to saturate binding of the FITC-casein (C and D), and thus these assays were carried out under "ligand depletion condition" (i.e. free [ATPγS] ≪ total [ATPγS]), which causes a shift in the apparent affinity of PAN for ATPγS compared to the actual affinity (Fig3).

D) The change in polarization of GFP-ssrA (0.08 μM) by PAN at different ATPγS concentrations.

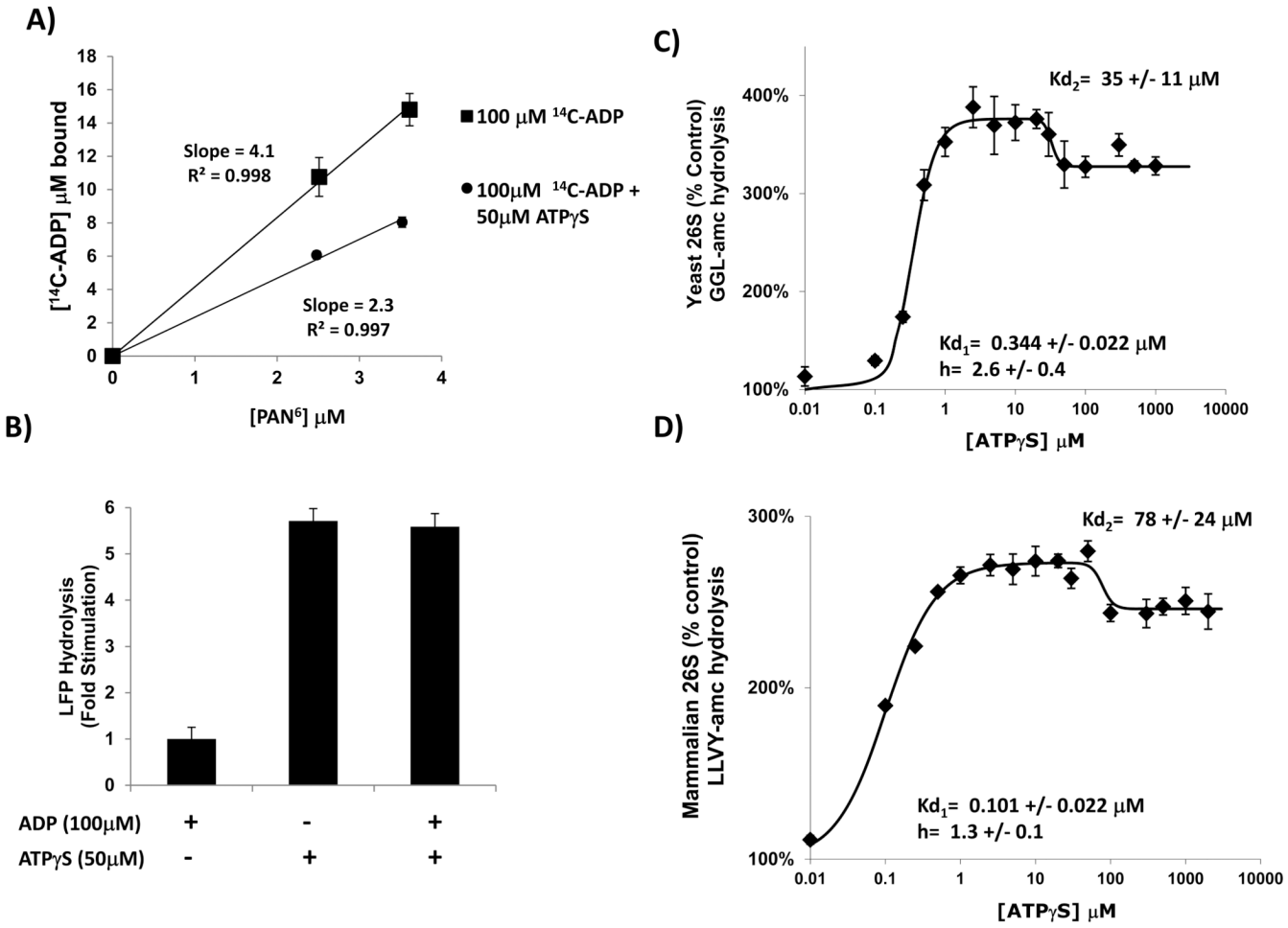

Figure 5. PAN functions optimally with 2 ATPγS and 2 ADP bound and gate-opening in the 26S proteasome shows similar multiphasic dependence on ATPγS as the PAN-20S complex with similar ATPγS affinities

A) 100μM of ^{14}C ADP was mixed with different concentrations of PAN with or without 50 μM of ATPγS (2-bound state). The amount of bound ^{14}C-ADP was determined as in Fig 2A. See also Figure S2.

B) The extent of gate-opening by PAN was determined by assaying LFP hydrolysis by the PAN-20S complex in the presence of the indicated nucleotides.

C) The rate of GGL-amc (20μM) hydrolysis by yeast 26S proteasomes (2μg/ml) at different ATPγS concentrations.

D) The rate of suc-LLVY-amc (100μM) hydrolysis by rabbit 26S proteasome (1μg/ml) was monitored at increasing concentrations of ATPγS.

See also Figure S1.

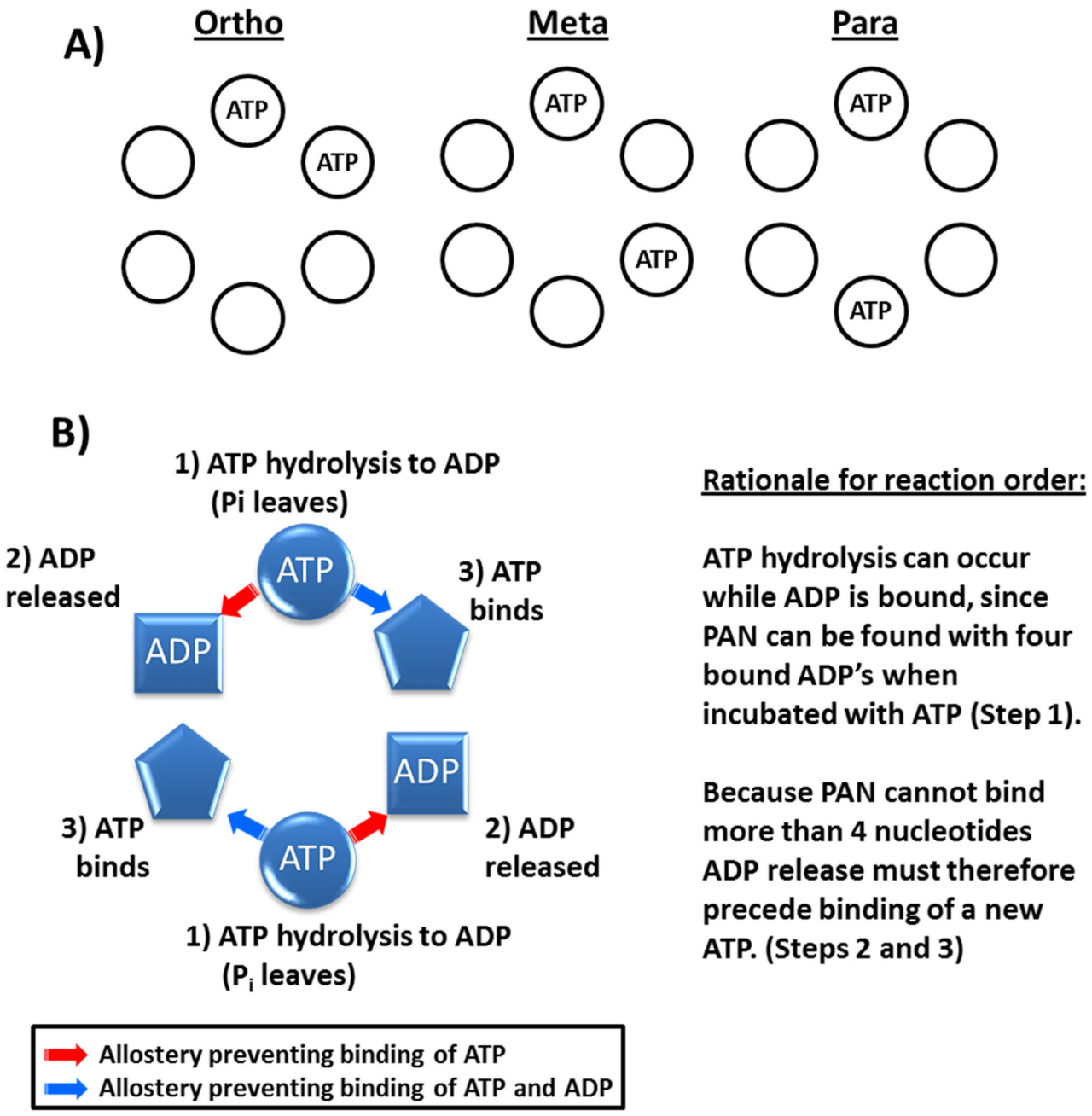

Figure 6. Nucleotide binding exchange model for the proteasomal ATPases

A) Three possible patterns by which a pair of ATP molecules can bind to a hexameric ring.

B) A model describing the binding-exchange reaction for the proteasomal ATPases based on the two cooperatively-linked para-positioned subunits binding ATP. Each subunit would cycle through ATP bound, ADP bound, and nucleotide-free states. The resulting ATP hydrolysis cycle is expected to occur in the clockwise direction in the order shown. See text for rationale.

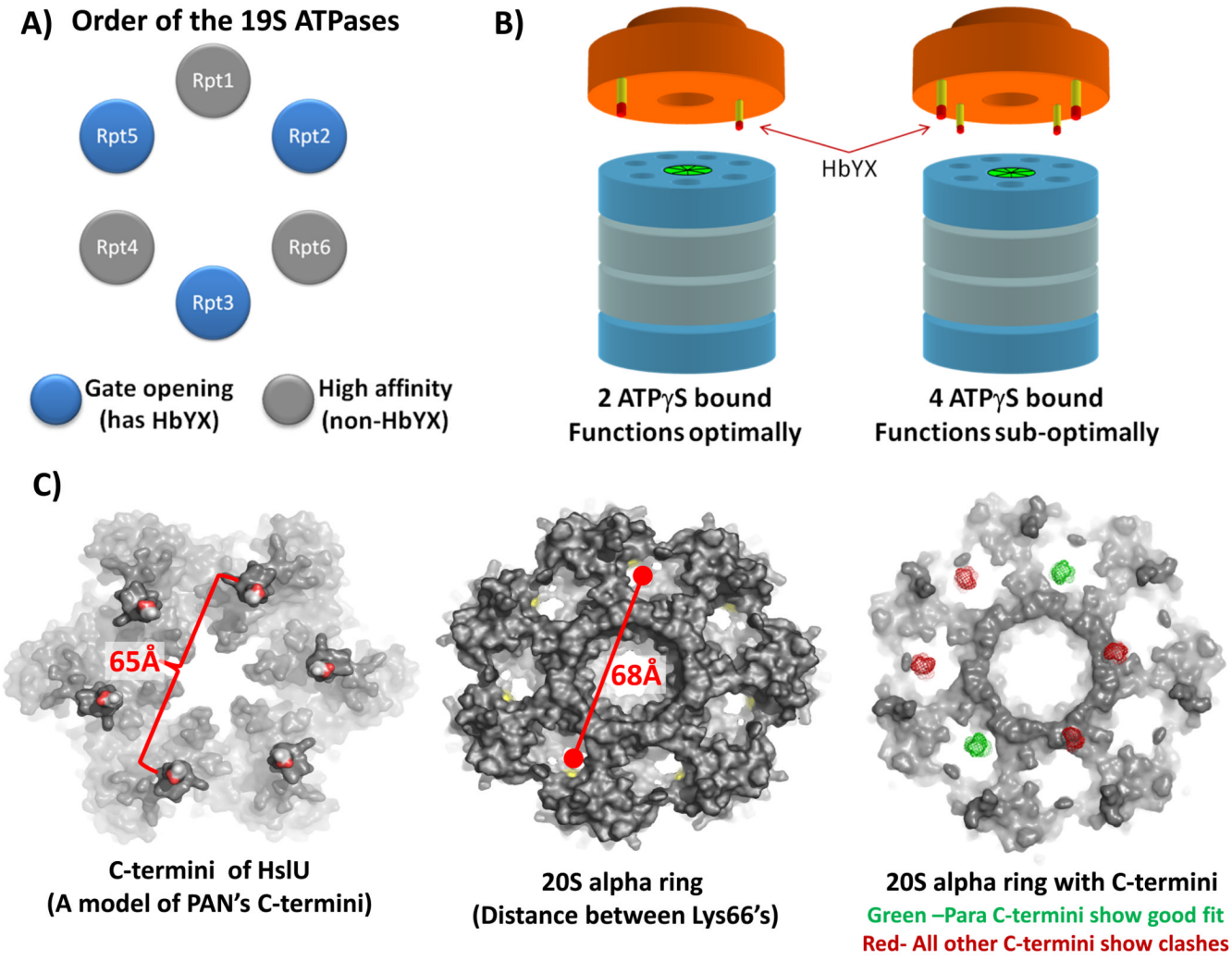

Figure 7. A sterically plausible model for how the hexameric para-positioned ATPase subunits interact with the heptameric 20S α- ring and why the 4-bound state reduces function

A) The order of the eukaryotic ATPases showing the alternating order of the HbYX and non-HbYX subunits.

B) Because ATP binding to PAN drives PAN-20S association, and because only two para subunits bind ATP, it's likely that only these two para C-termini interact with the 20S pockets at any instant. When 4 ATPγS bind, it's likely that 4 C-termini are extended to dock with the 20S, but this form has a reduced 20S affinity, probably caused by steric problems (see 4C).

C) X-ray structures demonstrate how PAN's para positioned C-termini can dock into the 20S intersubunit pockets without steric hindrance. Because crystal structures with PAN's C-termini are not available, we used the structure of the PAN homolog HslU as a model. The distance between carboxy groups on para C-termini (left), and the Lys66 γ- amine group in the indicated 20S intersubunit pockets (middle) are compatible as shown by manual docking HslU's para C-termini to the 20S α-ring (right), which shows the para C-termini (green) docked into two pockets without clashes. In this mode the other (non-para) C-termini (Red) would clash with residues in the 20S. Surface rendered structures and distance calculations were generated with Pymol (DeLano Scientific).